FORSCHUNGSZENTRUM
ROSSENDORF e.V.

FZR

FZR-72
February 1995
Preprint

B. Kämpfer, O.P. Pavlenko, A. Peshier and G. Soff

Parton kinetics for strangeness and charm production

Forschungszentrum Rossendorf e.V.
Postfach 51 01 19 · D-01314 Dresden
Bundesrepublik Deutschland

Telefon (0351) 591 3258
Telefax (0351) 591 3700
E-Mail kaempfer@gamma.fz-rossendorf.de

Parton kinetics for strangeness and charm production[1]

B. Kämpfer[a,b], O. P. Pavlenko[a,c], A. Peshier[a,b], G. Soff[b]

[a] *Forschungszentrum Rossendorf e.V., PF 510119, 01314 Dresden, Germany*
[b] *Institut für Theoretische Physik, Technische Universität Dresden, Mommsenstr. 13, 01062 Dresden, Germany*
[c] *Institute for Theoretical Physics, Kiev, Ukraine*

Strangeness and charm degrees of freedom are considered on the partonic level. First we present a model of the fully equilibrated quark-gluon plasma with thermal parton masses and find a considerable contribution of strangeness and also some charm. Then the kinetics of chemical equilibration processes of in an early hot glue system is modelled, i.e., the cooking of light and strange quarks in an expanding gluon gas is followed. The degree of equilibration depends on uncertainly known rates, however, we find that such penetrating probes as hard photons are less sensitive to details of the equilibration. Finally, we estimate the very early charm production in not yet thermalized parton matter and find indications for a clear dominance of the glue fusion processes, i.e., charm probes likely the early glue distribution.

INTRODUCTION

In ultrarelativistic heavy-on collisions (say at RHIC or LHC energies) the subnuclear degrees of freedom, i.e., quarks and gluons or partons, are expected to dominate the early dynamics. After loosing the coherence of partons, which are initially described by the nuclear structure functions, the very early stage of the collision dynamics is characterized by entropy production and secondary particle production. Due to the larger gluon-gluon cross sections the gluons are estimated to exceed the quark and anti-quark numbers in the charge-symmetric midrapidity region (1). Therefore, the thermalization processes in the hot glue, with a few quarks and anti-quarks immersed, should proceed on rather short time scales. Later on also the quark component can thermalize. But even if thermalization is achieved to some degree, chemical equilibration processes usually need longer time scales. Kinetic models, such as the parton cascade model (2) or the HIJING code (3), predict indeed approximate early thermalization but chemical off-equilibrium. Supposed the chemical equilibration is fast enough, the parton system evolves towards a quark-gluon plasma

[1]Supported by BMFT grants 06DR107 and 06DR666 I(4).
Invited talk at "Strangeness'95", Tuscon, Arizona, January 4 - 6, 1995.

(QGP), which hadronizes afterwards.

In the present paper we focus on three of the mentioned stages of parton matter evolution. We consider, going backwards in time,

(i) the QGP within a model with thermal parton masses and analyze the rôle of strange and charm quarks; this stage relies on the assumption of thermal and chemical equilibrium,

(ii) the chemical equilibration processes in an initially undersaturated gluon gas and follow in particular the cooking of strangeness in the hot glue; for such considerations the thermal equilibrium is supposed,

(iii) the thermalization process and address the question whether early charm production can probe this stage.

The aim of such investigations is to understand on a qualitative level relevant subprocesses in the rather involved evolution of partonic degrees of freedom. We also calculate penetrating probes (dileptons in items (i, iii), photons in item (ii)) in order to elucidate how these ones are affected by peculiarities of the parton evolution.

THERMAL PARTON MASSES IN A STRANGE QGP

Recently the observation has been made (4,5) that the pure SU(3) gauge theory lattice data (6,7) can rather perfectly be fitted by a non-interacting quasi-particle model with effective thermal gluon mass

$$m^2(T) = \frac{1}{\Gamma_g} g^2(T) T^2, \quad g^2(T) = \frac{16\pi^2}{(16 - \frac{2}{3}N_f)\log\left(\frac{T+T_s}{T_c}\right)^2}. \qquad (1)$$

The running coupling g is phenomenologically regularized by the shift parameter $T_s = 0.023\, T_c$. $\Gamma_g = 3.3$ is astonishing near the high-temperature QCD prediction $3/(1 + \frac{1}{6}N_f)$ (8,9). Only the physical transversal gluon modes ($d_g = 16$) are to be included in the primary thermodynamical potential

$$p(T) = \frac{d_g}{6\pi^2} \int dk \frac{k^4}{\omega(k,T)} [\exp\{\frac{\omega(k,T)}{T}\} - 1]^{-1}, \; \omega(k,T) = \sqrt{m^2(T) + k^2}. \quad (2)$$

The energy density and entropy are self consistently calculated from the pressure $p(T)$ and look not as the usual ideal gas formulae. Using the somewhat involved dispersion relation for the transversal in-medium gluon modes in one-loop order (8,9), instead of the free one Eq. (2), one does not find a noticeable change of the thermodynamical quantities.

Lacking precise lattice data with fermions we extend our thermal mass model to the QGP as follows: the Fermi statistics is properly accounted for; the known flavor and color degeneracies are included; the thermal masses are

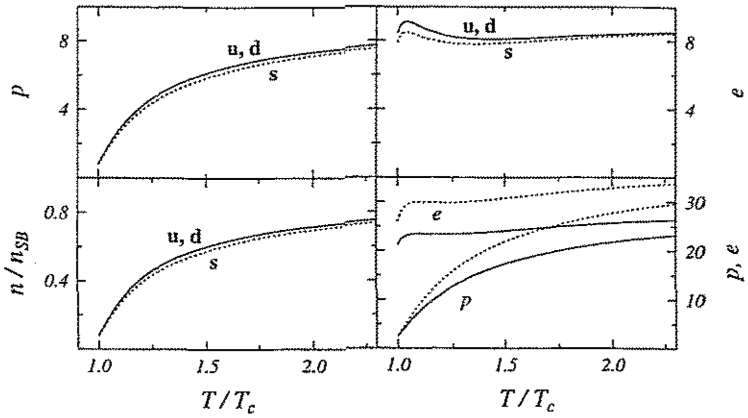

FIG. 1. The partial pressures (left upper panel, in units of $T^4 \frac{\pi^2}{90}$), the partial energy densities (right upper panel, in units of $T^4 \frac{\pi^2}{30}$), the partial particle densities (left lower panel, in units of the Stephan Boltzmann values), and the total energy density and pressure (right lower panel, full/dotted lines - 2/3 flavor plasma with the same $p(T_c)$).

as in high-temperature QCD, i.e., $\Gamma_Q = 6$; finite quark rest masses m_o give rise to expressions like $m = \sqrt{m_0^2 + m^2(T)}$ for the effective mass. The resulting equation of state is displayed in Fig. 1. One observes that the strange quarks behave in this model very much as the u,d quarks. This is to be contrasted with the bag model parametrization, where strangeness is suppressed, and the u,d quarks are taken as in the Stephan Boltzmann limit, and e/T^4 is an overall decreasing function. The local maximum of our quark energy density resembles recent two-flavor lattice results (10).

When including also charm (but leaving $N_f = 3$ in the above quoted equations) we find at least a 10% contribution to the thermodynamical quantities shown in Fig. 1. Therefore, if our model equation of state is correct and the numerical values of the decisive values of $\Gamma_{g,Q}$ are near the high-temperature one-loop QCD calculations also charm contributes to a fully equilibrated QGP and should be included properly in precision lattice calculations.

There are distinct observable effects of finite thermal masses. For example, the $M_\perp$ scaling property of the dilepton spectrum is violated (11). A detailed analysis (5) shows the appearance of a threshold effect in the transverse-mass spectrum at transverse dilepton momentum $q_\perp = \sqrt{M_\perp^2 + m^2(T)} \to M_\perp$. In this region the dilepton production is strongly suppressed (5). Also the cooling behavior of the QGP is changed; this stems from the fact that the latent heat in the present model is much smaller than in the bag model. Another consequence is the higher temperature at given entropy density. This in turn affects estimates of rates at given particle rapidity densities.

CHEMICAL EQUILIBRATION PROCESSES IN AN EXPANDING QGP

Qualitative estimates and parton cascade simulations indicate substantial quark undersaturation (1–3,12,13) at early times in the course of an ultra-relativistic heavy-ion collision; in the same moment the gluon distribution looks isotropically and can be considered as thermalized. To follow the chemical equilibration processes in the hot glue one can formulate rate equations (14). Here we utilize rate equations similar to those used in Refs. (12,15). The change of densities of different particle species obeys the master type equations

$$\hat{n}_g = \frac{1}{2}\,\bar{\sigma}_{gg\to ggg}\,n_g^2\,(1-\lambda_g) - \bar{\sigma}_{gg\to q\bar{q}}\,(n_g^2 - n_q^2\,b) - \bar{\sigma}_{gg\to s\bar{s}}\,(n_g^2 - n_s^2\,\tilde{b}), \quad (3)$$

$$\hat{n}_q = \frac{1}{2}\bar{\sigma}_{gg\to q\bar{q}}\,(n_g^2 - n_q^2\,b) - \frac{1}{2}\bar{\sigma}_{q\bar{q}\to s\bar{s}}\,(n_q^2 - n_s^2\,c), \quad (4)$$

$$\hat{n}_s = \frac{1}{2}\bar{\sigma}_{gg\to s\bar{s}}\,(n_g^2 - n_s^2\,\tilde{b}) + \frac{1}{2}\bar{\sigma}_{q\bar{q}\to s\bar{s}}\,(n_q^2 - n_s^2\,c), \quad (5)$$

where

$$\hat{n} \equiv \dot{n} + \frac{n}{\tau} + n\,\frac{\dot{<\gamma>}}{<\gamma>} \quad (6)$$

is the comoving derivative of particle density which includes boost invariant longitudinal and transversal expansion (γ is the transverse Lorentz factor, cf. Ref. (15); $\dot{}\ = d/d\tau$, and τ is the proper time). The thermally velocity-averaged cross sections $\bar{\sigma}_{...}$ account for inelastic glue production, glue flows into u,d channel, glue flows into s channel, u,d production from glue, u,d flow into s channel, glue flows into s channel, u,d transmutates into s and the corresponding back reactions. The remaining quantities $b \equiv \frac{\tilde{n}_g^2}{\tilde{n}_q^2}$, $\tilde{b} \equiv \frac{\tilde{n}_g^2}{\tilde{n}_s^2}$, $c \equiv \frac{\tilde{n}_q^2}{\tilde{n}_s^2}$ are so defined that in equilibrium the reactions cease. A tilde indicates the corresponding saturation density, e.g., $\lambda_g = n_g/\tilde{n}_g$ is the gluon fugacity. These coupled three equations are supplemented by one equation for energy conservation, and two equations for transverse expansion (for details cf. Ref. (15)). We solve this system with the following simplifications: neglecting the $q\bar{q} \to s\bar{s}$ channel (14), and using $\sigma_{gg\to q\bar{q}} = 2\,\sigma_{gg\to s\bar{s}}$ (this neglects the mass difference of u,d and s quarks, see previous section, as also done in $\tilde{n}_s$, energy density, and pressure). These simplifications seem to be harmless compared to uncertainties in the thermally averaged cross sections and higher order processes (16). We use here the cross sections of Ref. (12) in one set of calculations (set I), and in a second set we multiply these cross sections by a factor 10 (set II). The initial conditions are also matter of debate (cf. refs. (1,12,13,15,16) for widely differing estimates).

In Fig. 2 two representative examples are displayed. In both ones the u,d quarks are initially undersaturated, while the gluons are either undersaturated too (12,13,16) or even oversaturated (17). We assume that there is initially no

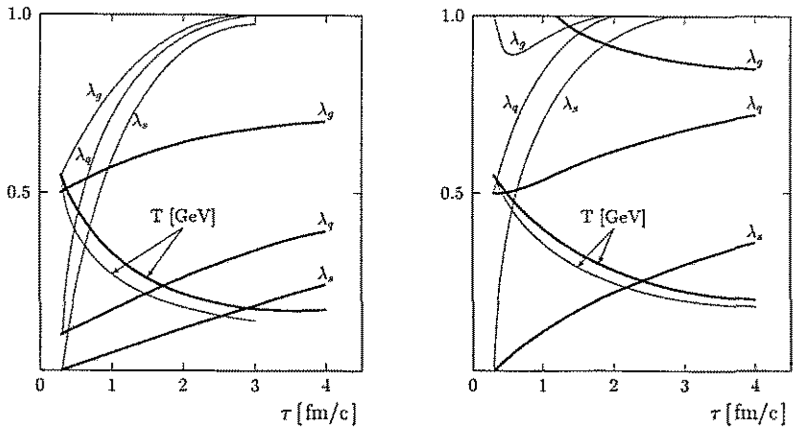

FIG. 2. Time evolution of the temperature and the various fugacities for two different initial conditions (heavy/thin curves - set I/II calculations). The initial transverse expansion velocity is zero, and the transverse radius is 5 fm. Transverse expansion is dealt with by exploiting the global relativistic hydrodynamics Ref. (15).

strangeness. One observes that in the set I calculation the system remains far from chemical equilibrium. If gluons are initially rare the glue production is not efficient enough to overcompensate the gluon loss in the $gg \to q\bar{q}, s\bar{s}$ reactions. The strange channel, which is not included in the previous calculations (12,15), mainly reduces the gluon fugacity, while for the temperature and light quark fugacities it is not so important. Our set II calculation displays fast approach to equilibrium even in the strangeness channel.

We mention that we do not include the $g \to q\bar{q}, s\bar{s}$ reaction channel. When utilizing the thermal masses of the previous sections, this channel is closed. Giving the particles, however, a width then via the tails of the distributions such reactions can proceed, cf. Ref. (18). Our thermal masses have some support from the lattice calculations; the estimates of the particle decay widths rely completely on the extrapolation from the high-temperature evaluations.

While the drastically different flavor evolution scenarios I and II demonstrate the need to constrain the reaction cross sections, as also the initial conditions, one may investigate whether penetrating probes are sensitive to such differences. In Ref. (15) we have calculated the photon spectra for $p_\perp^\gamma >$ 1 GeV. We found that the slopes are rather insensitive to the different flavor evolutions. The decisive quantities, which nearly completely determine the photon spectra, are the poorly known initial temperature and fugacities.

One might also include the charm evolution in the above master equations. Recent estimates (13), however, indicate that the pre-equilibrium contribution is much larger than the thermal rate.

The proper inclusion of in-medium effects in the kinetic treatment of flavor evolution needs obviously more investigations too.

PARTON KINETICS FOR CHARM PRODUCTION

Hard probes come from early stages of the parton evolution (19,20). Therefore, one has to look at heavy particles to learn about early parton distribution evolution. Here we are going to present an analytical model for the early off-equilibrium parton kinetics and estimate the charm production. Previous estimates (13,21) rely on parametrizations of HIJING results. We adopt the Boltzmann equation in relaxation time approximation for the one-dimensional boost invariant evolution of the parton distribution function f

$$(\partial_\tau - \frac{\mathrm{th}\xi}{\tau}\,\partial_\xi)\,f = \tau_{rel}^{-1}\,(u_\mu p^\mu)\,(f - f_{eq}), \tag{7}$$

where τ and ξ are proper time and rapidity, and τ_{rel} denotes the relaxation time. The fiducial distribution f_{eq} is the usual Jüttner function needed for linearizing the collision operator. The four-velocity flow pattern u_μ is prescribed by the symmetry of the system. p^μ is the parton four momentum. The remaining temperature parameter in f_{eq} is determined by an integral equation (cf. Ref. (19) for technical details) and depends on the initial distribution $f_0 = f(\tau_0)$. The exact solution

$$f(\tau) = f_0(\tau)\,\exp\left\{\frac{\tau_0 - \tau}{\tau_{rel}}\right\} + f_{eq}\,[1 - \exp\left\{\frac{\tau_0 - \tau}{\tau_{rel}}\right\}] \tag{8}$$

might be used, e.g., for the charmed pair production rate

$$\frac{dN_{c\bar{c}}}{d^4x} = \int dM^2\,\frac{d^3p_1}{(2\pi)^3}\frac{d^3p_2}{(2\pi)^3} f(p_1)\,f(p_2)\,\sigma(M^2)\,v_{rel}\,\delta([p_1+p_2]^2 - M^2) \tag{9}$$

with standard cross sections (14) $\sigma = \sigma_{gg\to c\bar{c}} + \sigma_{q\bar{q}\to c\bar{c}}$.

As an aside we mention that such an approach has been exercised for dileptons with $\sigma = \sigma_{q\bar{q}\to\mu^+\mu^-}$. Also in this case there are three terms in the rate

$$\frac{dN_{\mu^+\mu^-}}{d^4x} \propto f_0^2 + 2\,f_0\,f_{eq} + f_{eq}^2, \tag{10}$$

and we found (22) that, unless the relaxation time is extremely short, the term $\propto f_0^2$ dominates, i.e., hard probes measure indeed the initial distributions.

An analog calculation for charm is not yet performed. Instead we utilize a simplified 2-component model, where the gluons are thermalized, $f_g = f_g^{eq}$, while the quarks are not thermalized, $f_q = f_q^0$. In case of $f = f_{eq}$ one recovers the thermal rate (cf. Refs. (22,23) for further explanations)

$$\frac{dN_{xx\to c\bar{c}}}{dM^2\,dY} \propto \frac{\lambda_x^2\,\bar{\sigma}_{xx\to c\bar{c}}}{M^2}(T_0^3\tau_0)^2[H(\frac{M}{T_0}) - H(\frac{M}{T_c})], \tag{11}$$

where the "x" means g. To compare this thermal rate with a non-thermal one, we use the evolution equation Eq. (8) but neglect the f_{eq} component (see the

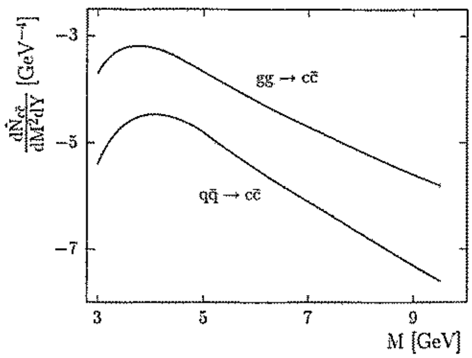

FIG. 3. The charm pair spectrum (in units of $\pi(\alpha_s R n_0 \tau_0)^2$; $\tau_0 = \hbar c/p_\perp^*$; R is the transverse area (22)) as function of invariant mass M.

above remark on dileptons). The quarks obey initially a mini-jet produced parton distribution

$$f_0(p_\perp, y, \tau_0) = \mathcal{N}\,\Theta(p_\perp - p_\perp^*)\,\delta(y)\,p_\perp^{-l}, \quad l \approx 7, \quad p_\perp^* = 2\,\mathrm{GeV}. \qquad (12)$$

The corresponding rate Eq. (9) for quarks ("x" stands for q or $\bar{q}$)

$$\frac{dN_{xx\to c\bar{c}}}{dM^2\,dY\,dq_\perp} \propto \sigma_{xx\to c\bar{c}}\,M^2\lambda_x^2 \int d\tau\,\tau\,[f_0^2(\tau)\cdots] \qquad (13)$$

can be simplified somewhat, cf. Ref. (22). To compare the charm yields from thermalized gluons and not yet thermalized quarks we normalize the corresponding distribution functions f_{eq} and f_0 on the same energy densities and particle densities, i.e., $e_{eq} = e_0$ and $n_{eq} = n_0$. This relates the parameters in both distributions, in particular it causes a rather high initial temperature T_0 of the hot glue (22). Interestingly, the spectra for $gg \to c\bar{c}$ and $q\bar{q} \to c\bar{c}$ look very similar, see fig. 3. However, due to the low quark fugacities (here we assume $\lambda_q \sim \frac{1}{5}\lambda_g$ in line with Refs. (1,12,13,16)) the rates behave as

$$\frac{N_{q\bar{q}\to c\bar{c}}}{N_{gg\to c\bar{c}}} \propto \left(\frac{1-x}{x}\right)^2, \qquad (14)$$

where $x = 1 - \frac{n_{q+\bar{q}}}{n_{q+\bar{q}+g}}$ (which means in full chemical equilibrium $x_{eq} = 0.4$). The present fugacities imply a strong quark undersaturation, i.e., $x \sim 0.8$, which results in a suppression factor $\frac{1}{37}$ for light quark-created charm. We mention that roughly the same results are obtained if quarks would be thermalized too, or if the gluons also obey the mini-jet initial distribution). That means, charm measures the gluon initial distribution.

While the model needs improvements for handling thermalization and chemical equilibration together, it might be sufficient for qualitative estimates and for comparison with initial gluon fusion (13,21).

SUMMARY

Our results may be summarized as follows:

(i) If the thermal mass model is correct then s quarks behave nearly as u,d quarks; there is no need of a bag constant; the latent heat is much smaller than in the bag model.

(ii) The chemical flavor evolution depends sensitively on the cross sections for gluon multiplication $gg \to ggg$, quarkization $gg \to q\bar{q}$ and $gg \to s\bar{s}$, and quark transmutation $q\bar{q} \to s\bar{s}$; either strangeness remains, as u,d quarks, undersaturated, or s gets similar to u,d saturated. Penetrating probes, e.g., photons do not depend on these differences.

(iii) If quarks are really strongly suppressed in the early stages then charm probes the initial (pre-equilibrium) gluon distribution f_g^2 (from other studies ones knows that photons probe $f_g\, f_q$, and dileptons f_q^2).

REFERENCES

1. E. Shuryak, L. Xiong, Phys. Rev. Lett. **70**, 2241 (1993).
2. K. Geiger, Phys. Rev. D **47**, 133 (1993), D **48**, 4129 (1993), Phys. Rep. in print.
3. X.N. Wang, M. Gyulassy, Phys. Rev. D **44**, 3501 (1991).
4. W. Greiner, D. Rischke, Columbia preprint CU-TP-648 (1994).
5. A. Peshier, B. Kämpfer, O.P. Pavlenko, G. Soff, Phys. Lett. B **337**, 235 (1994).
6. J. Engels et al., Phys. Lett. B **252**, 625 (1990).
7. D. Rischke et al., Phys. Lett. B **278**, 19 (1992); Z. Phys. C **56**, 325 (1992).
8. V.V. Klimov, Sov. Phys. JETP **55**, 199 (1982).
9. H.A. Weldon, Phys. Rev. D **26**, 1394, 2789 (1982).
10. T. Blum, L. Kärkkäinen, D. Tousaint, S. Gottlieb, preprint AZPH-TH/94-22.
11. B. Kämpfer, O.P. Pavlenko, Phys. Rev. C **49**, 2716 (1994).
12. T. Biro et al., Phys. Rev. C **48**, 1275 (1993).
13. P. Levai, B. Müller, X.N. Wang, preprint LBL-35981.
14. P. Koch. B. Müller, J. Rafelski, Phys. Rep. **142**, 167 (1986).
15. B. Kämpfer, O.P. Pavlenko, Z. Phys. C **62**, 491 (1994).
16. L. Xiong, E. Shuryak, Phys. Rev. C **49**, 2207 (1994).
17. K. Geiger, J.I. Kapusta, Phys. Rev. D **47**, 4905 (1993).
18. T. Altherr, D. Seibert, Phys. Lett. B **313**, 149 (1993); Phys. Rev. C **49**, 1684 (1994);
    N. Bilic, J. Cleymans, I. Dadic, D. Hiskop, preprint BI-TP-94/36.
19. B. Kämpfer, O.P. Pavlenko, Phys. Lett. B **289**, 127 (1992).
20. K. Geiger, J.I. Kapusta, Phys. Rev. Lett. **70**, 1920 (1993).
21. B. Müller, X.N. Wang, Phys. Rev. Lett. **68**, 2437 (1992).
22. B. Kämpfer, O.P. Pavlenko, FZR-93-16, Nucl. Phys. A **566**, 351c (1994).
23. A. Shor, Phys. Rev. Lett. **48**, 1597 (1982); Phys. Lett. B **154**, 1122 (1985).